J. exp. Biol. (1978), **72**, 251–260
With 8 figures
Printed in Great Britain

MECHANICAL PROPERTIES OF PRIMARY FEATHERS FROM THE PIGEON

BY P. P. PURSLOW AND J. F. V. VINCENT
Biomechanics Group, Department of Zoology, Reading University

(*Received* 30 *June* 1977)

SUMMARY

The morphology of the primary feather shaft from the pigeon wing has been examined and its salient features noted. The cortex (outer wall) of the shaft appeared to be the most significant feature in relation to bending behaviour and was analysed quantitatively. A model that simulated bending of the shaft was made using this analysis and upon comparison of simulated results with observed bending behaviour it is shown that the shape and size of the cortex does indeed account for the majority of bending behaviour. The model does not include torsional effects and the effects of the pithy medulla and the transverse septa, but the magnitude of these effects is considered to be small in comparison with that of the cortex considered in simple bending. Differences in the shape of the cortex in the outermost primary and those proximal to it are shown to account for different mechanical properties and possible reasons for this are given. The shape and size of the cortex, as measured by its second moment of area, is shown to have some relation to the body weight of the bird.

INTRODUCTION

The primary feathers of the pigeon (*Columbia livia*) are subjected to aerodynamic forces during flight and the feather shaft reacts by bending under these loads. The relationship between the structure of the shaft and its bending behaviour has been studied only superficially. The bending of feathers is discussed briefly by Alexander (1968) in his description of a bird's wing, and the morphology of the feathers from several species of birds was examined in great detail by Rutschke (1966), but he related shaft structure to mechanical function in a descriptive fashion, with little quantitative analysis. In this paper the morphology of the shaft is quantitatively related to its mechanical properties according to the following considerations.

When a cantilever such as that in Fig. 1 is subjected to a load it is deflected and tensions and compressions are set up within it. At some points in the beam neither tension nor compression exists, and the line joining all these points is referred to as the neutral axis of the beam. The ability to resist the effects of bending loads applied to a beam of a given cross-section is dependent upon three things: the amount of material in the cross-section available to withstand loading, the stiffness of the material and the distribution of the material about the neutral axis of the section. The first and last things are measured by the second moment of area of the section, I, which attaches more significance to material further away from the neutral axis than

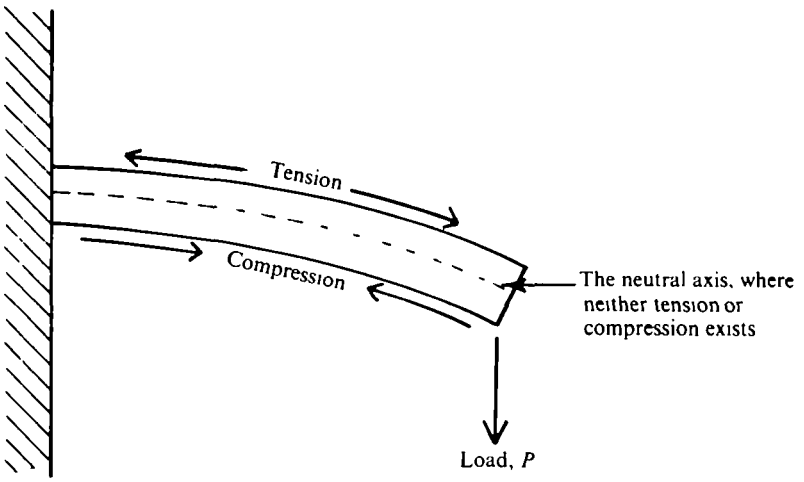

Fig. 1. Bending of a cantilever. A feather is structurally a cantilever, the base being inserted into the skeleton of the wing.

to material close to it. (For an extensive explanation of the significance of I see Wainwright *et al.* (1976)). In order to be able to calculate I the position of the neutral axis has to be determined and this is done by calculating the first moment of area of the section.

If the Young's Modulus, E, and the second moment of area, I, of the beam are known, deflexions caused by applied loads can be calculated using beam theory. We thought that the bending behaviour of the feather shaft would be dominated by the effects of the cortex, and that internal material and structures had no significant effect. If this were so it could be tested by measuring E and I for the cortex of the shaft and calculating the deflexions under load as governed by these parameters. These could then be compared to actual deflexions obtained in the feathers when loaded.

MATERIALS AND METHODS

Feathers from the left and right wings of five pigeons (*C. livia*) were used. The body weights of the birds chosen were 265, 280, 300, 400 and 460 g.

Shaft morphology

The outermost feather from the left wing of all five birds, and the four feathers proximal to the outermost feather on the left wing of the 300 g bird, were used here. Each feather shaft was measured, marked off at intervals along its length, and the small sections of shaft carrying these marks were dehydrated in a series of alcohols before being embedded in Araldite. Each embedded section was cut, wet-ground and polished down to the mark. Deviations from perfectly normal sectioning were allowed up to 15° on the basis that the percentage error in area estimation at 15° from normal is $((1/\cos 15°)-1)\times 100\%$ for elliptical or rectangular sections, which works out to an error of 3·5%. Errors up to this level were considered to be reasonable. An angle of 15° from normal is easily discernible by eye. These cross-sections wer

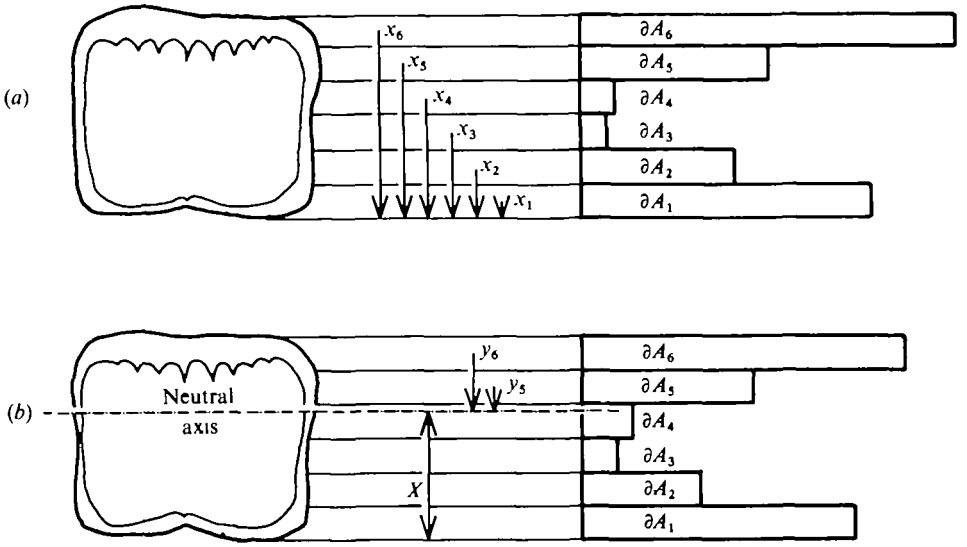

Fig. 2. (*a*) First moment of area calculation. The cortex is divided into strips. The area of cortex in each strip, A_i, and the distance (x_i) of the centroid of each area from an arbitrary baseline is measured. (*b*) Second moment of area calculation. The position of the neutral axis is taken from the first moment of area. The distance from the neutral axis to each centroid of area, y_i is measured.

photographed together with a scale, and traced onto graph paper for the following analyses.

Second moment of area calculation

The *first moment of area of the cortex* was calculated as follows (see Fig. 2*a*):

The first moment of area, XA, is given by:

$$XA = \sum_{i=0}^{i=6} A_i . x_i, \tag{1}$$

where X is the quantity required from the calculation, and is the distance from an arbitrary baseline to the neutral axis of the section. The total area of the cortex, A, was also noted for each section.

The *second moment of area* may now be calculated (see Fig. 2*b*). Subtract the distance X from x_1 to x_6 to give y_1 to y_6, which are the distances (+ve or −ve) from the neutral axis to the centroid of each area.

The second moment of area, I, is then given by:

$$I = \sum_{i=0}^{i=6} y_i^2 . A_i. \tag{2}$$

I values were calculated for each section in a vertical plane (horizontal strips, to give I_{xx}, a measure of resistance to dorso-ventral bending) and in a horizontal plane (vertical strips, to give I_{yy}, a measure of resistance to lateral bending).

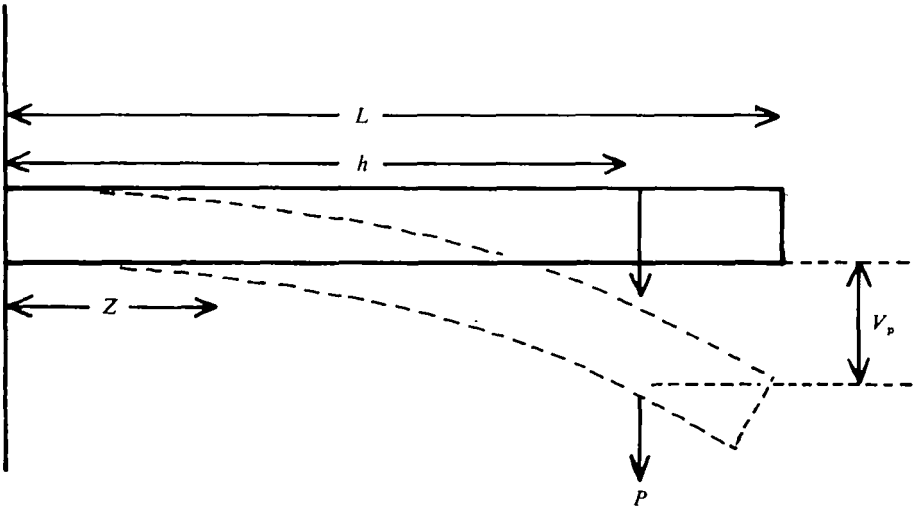

Fig. 3. Deflexion in a cantilever beam under static point load.

Bending tests

The five outermost primaries from the right wing of the 300 g bird were measured and their shafts marked at regular intervals. The base of each shaft was glued into an aluminium alloy block held rigidly in a solid stand. Deflexions caused by suspending a given load (26·93 g) from the shaft at each mark were measured at the point of loading for two shaft orientations:

(i) shaft horizontal with dorsal surface uppermost;

(ii) shaft horizontal with leading lateral surface uppermost.

Mathematical model

In a beam (Fig. 3) of length L and stiffness E, fixed at one end and loaded at some distance h from the fixed end, the deflexion at the point of loading, V_p, is given by:

$$V_p = P \int_0^h \frac{h - z^2}{EI}\, dz, \tag{3}$$

where z is any distance between 0 and h.

The I_{xx} and I_{yy} values calculated from the sections of shaft were used to simulate deflexions at the same points and under the same load as in the actual bending tests, so that direct comparison between observed and calculated deflexions was possible. The E values used were based on previous extension tests on strips of feather shaft cortex, and were adjusted for best fit.

Effects of medulla removal

A test length (5 cm) was cut from the middle of nine primary feather shafts and the ends of each piece glued into aluminium alloy end pieces. These preparations were tested in dorso-ventral and lateral three point bending on an Instron testing machine, table model 1026, using loads that did not exceed the elastic limit of the specimen. A wide-bored hypodermic needle was then used to bore out the medulla and septa of each test piece and the tests in dorso-ventral and lateral orientations were repeated.

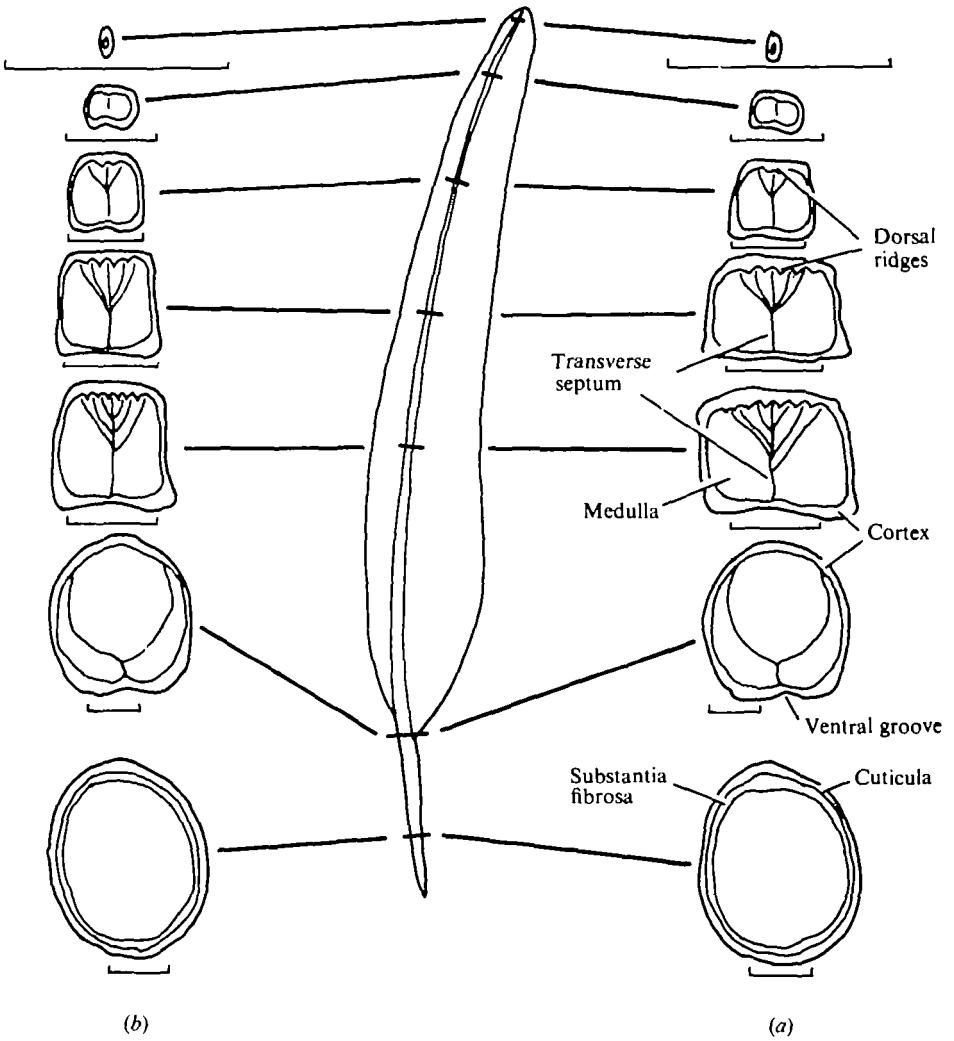

Fig. 4. Generalized cross-sections through the shaft at various points along its length for (*a*) the outermost feathers and (*b*) those proximal to the outermost feather. Scale lines 1 mm.

RESULTS

Morphology of shaft

The shaft (Fig. 4) is divided into two major regions, the rachis and the calamus, this division occurring at the superior umbilicus where the two regions blend smoothly into each other. The calamus is a hollow tube of only the cortical layers and is slightly elliptical in cross-section. The rachis, which bears the feather vane, is rectangular in cross-section and is filled by the substantia medullaris, which consists of multi-angular dead cells of varying size, with air-filled cavities. On the interior dorsal surface of the substantia fibrosa there are ridges of cortical material which run along two thirds of the rachis. Towards the base of the rachis there are six ridges. As the rachis becomes smaller towards its tip these do not converge, but the outer ridges

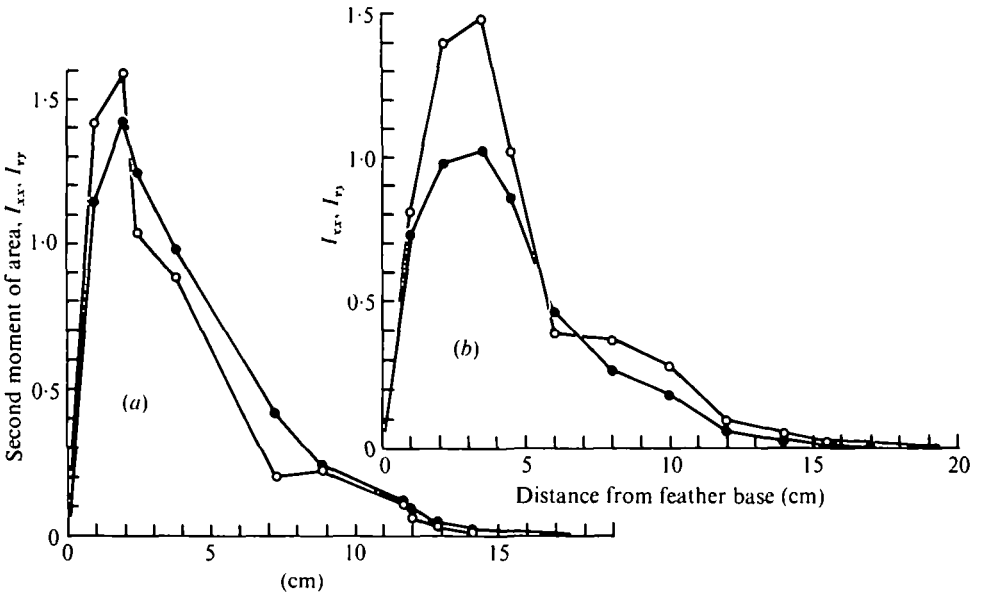

Fig. 5. Second moment of area values at distances along the shaft for (*a*) the outermost feather and (*b*) the feather immediately proximal to the outermost feather on the left wing of the 300 g bird. ○ = I_{xx} values; ● = I_{yy} values.

fade out, so that four, and then two ridges remain. These too fade out towards the tip of the rachis. Running in a dorso-ventral direction in the medulla are septa (transverse septa). These branch in mid-section, each branch running to a point midway between two dorsal ridges. As the ridges fade out so too does the number of branches of the septa. For the first two thirds of the rachis the lateral walls of the cortex are very much thinner than the dorsal and ventral walls. The ventral 'corners' of the section are much thickened and the distance between the lateral walls of the cortex is greater than that between the dorsal and ventral walls in the outermost feathers; for the four feathers proximal to the outermost the reverse is the case.

Towards the tip of the rachis the differences in thickness of the lateral and dorso-ventral walls of the cortex are lost and the section takes on the appearance of a solid circular tube of medulla in a rectangular cortex. Right at the tip of the feather the dorsal and ventral walls of the cortex are very much thicker than the lateral walls.

I values

Values of I_{xx} (dorso-ventral bending) and I_{yy} (lateral bending) at distances along the feather shaft are shown in Fig. 5 for the outermost feather and the feather immediately proximal to it from the left wing of the 300 g bird. The maximum I values occur at or around the point of insertion of the shaft into the skin of the wing and values decrease further along the shaft. This is as expected from beam theory.

Shaft bending behaviour

Fig. 6 shows deflexions obtained in the static beam loading experiment on the shafts of the outermost feather (Fig. 6*a*) and the feather immediately proximal to it

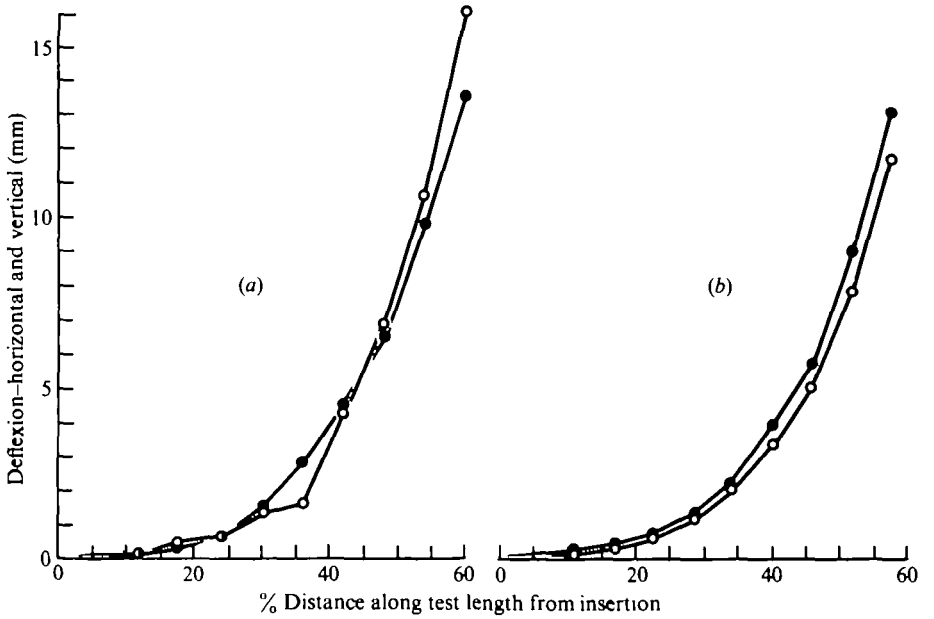

Fig. 6. Deflexions under static load applied at distances along the shaft for (*a*) the outermost feather and (*b*) the feather immediately proximal to it from the right wing of the 300 g bird. ○ = dorso-ventral bending; ● = lateral bending.

(Fig. 6*b*). The other three feathers yielded results very much like Fig. 6(*b*). The important point to note from these results is that the outermost feather is equally stiff laterally as dorso-ventrally, whereas the other feathers are much less stiff laterally than dorso-ventrally, although their dorso-ventral stiffness is much the same as that of the outermost feather.

Calculated deflexions

Calculated deflexions, for the same load applied at the same points along the shaft as used in the actual bending tests, are plotted against observed deflexions from the bending tests in Fig. 7 for the same two feathers as shown in Fig. 5. Perfect fit between observed and calculated data would result in the lines for bending in the two directions both lying along the straight dotted line at 45° to each axis. This plot gives a much easier interpretation of results than trying to compare curves.

Both Fig. 7(*a*) and (*b*) show a reasonable fit of the model with the observations, with lines for lateral and dorso-ventral bending being good approximations to straight lines. In the outermost feather (Fig. 7*a*) the shaft is consistently stiffer than expected dorso-ventrally, and in the other shaft (Fig. 7*b*) dorso-ventral deflexions are greater than expected.

Medulla removal

In all nine test pieces the loss in dorso-ventral flexural stiffness due to removal of the septa and medulla was consistently greater than the loss in lateral flexural stiffness. Loss of dorso-ventral stiffness was 16·1% ± 1·15% (mean ± S.E., sample size = 18)

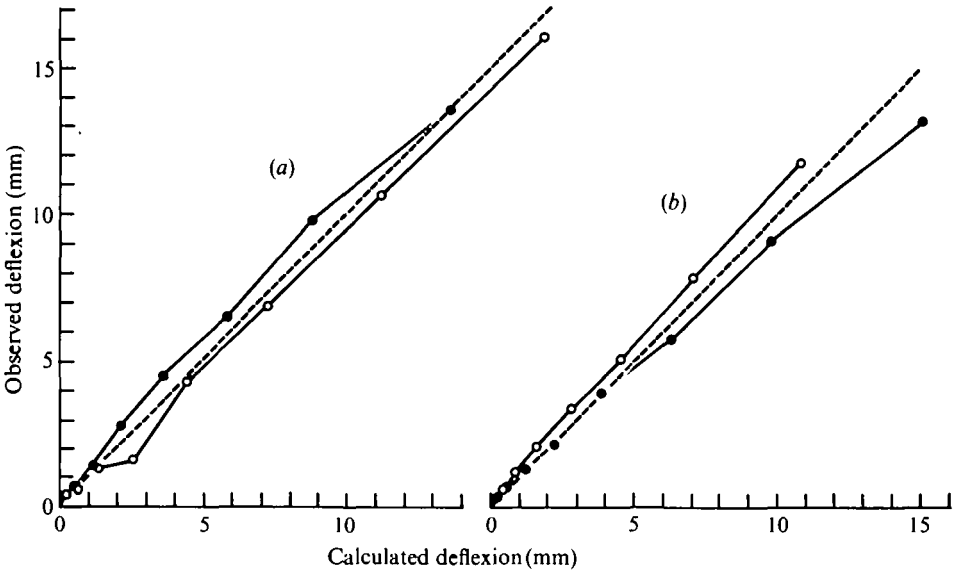

Fig. 7. Comparison between observed and calculated deflexions using equation (3) for the outermost feather (*a*) and the feather immediately proximal to it (*b*). The dotted line shows the line of perfect fit. Values of E used were: (*a*) $7{\cdot}75 \times 10^9$ Nm^{-2}; (*b*) 10^{10} Nm^{-2}. ○ = dorso-ventral bending; ● = lateral bending.

and the loss of lateral stiffness was $7{\cdot}8\% \pm 1{\cdot}97\%$ (mean ± S.E., sample size = 18). Thus, by inference, the effect of the medulla and transverse septa on dorso-ventral stiffness is about twice that on lateral stiffness.

DISCUSSION

The results of the calculations used to predict shaft bending under imaginary loads give a good fit to observed shaft bending, and therefore the calculations can be considered as a reasonable model of shaft behaviour in simple bending at the loads used. The calculations assume that the load-extension curve of the shaft is linear at the loads used. The curves obtained in the three point bending tests showed that this assumption is valid, as linear responses were obtained for all test pieces. Other assumptions are that the shaft is subject only to simple bending, and that only the cortex is mechanically important. These last two assumptions are not entirely correct and the small discrepancies in fit between observed and simulated deflexions may be attributed to these. In Fig. 7(*b*) the shaft is shown to be less stiff than predicted. As the shaft is not straight but slightly curved, dorso-ventral loading will result in some torsional deflexion as well as simple bending. If torsion were taken into account in the model this discrepancy could probably be accounted for. Outermost feathers, such as that in Fig. 7(*a*), seem to be somewhat straighter than those proximal to them and so torsion does not come into play as much. It was observed (Fig. 7*a*) that the shaft was stiffer than expected in the dorso-ventral direction. This can be attributed to the directional stiffening effect of the medulla and transverse septa (not

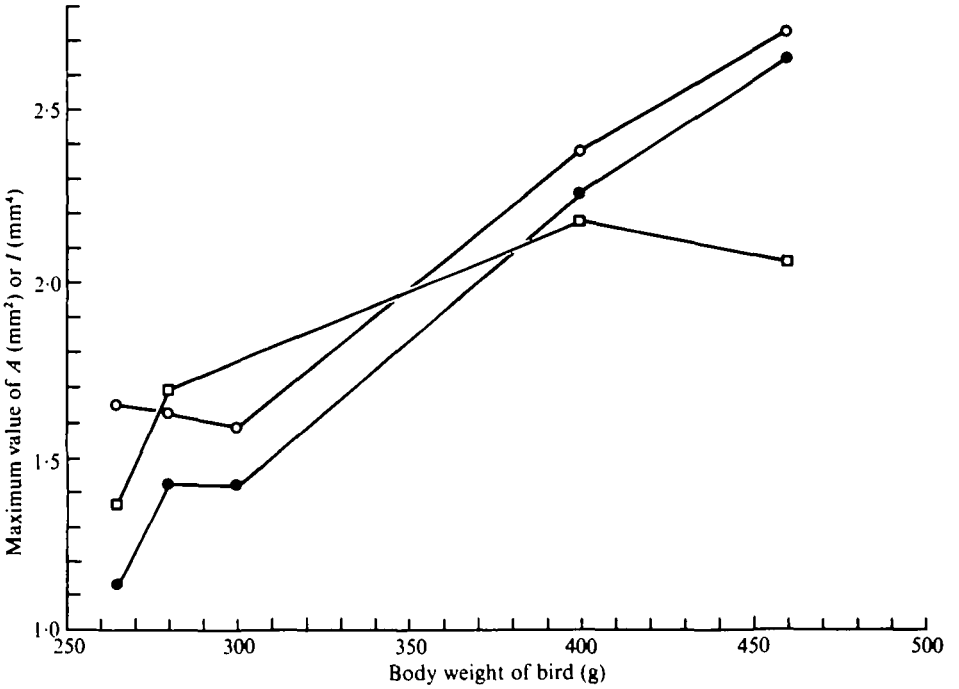

Fig. 8. Maximum I values and maximum area of cortex found in the shaft *v.* body weight of bird. ○ = I_{zz} max; ● = I_{yy} max; □ = A_{max}.

considered in the model). This effect, of course, is also in play in the feathers proximal to the outermost feather, but the magnitude of the effect is small and is probably obscured by torsional effects. Incorporation of these effects into the model presents problems in accurate morphological interpretation and as the increase in accuracy of the model would be only marginal, model refinement is thought to be unnecessary at present.

Heavier birds need to generate greater forces to keep them airborne than smaller birds, and this in turn means that the resistance to bending as measured by I_{xx} and I_{yy} should be greater in heavier birds. This can be seen to be the case in Fig. 8. The figure also shows a plot of maximum cross-sectional area of cortex against body weight. If the general cross-sectional shape of a shaft is fairly constant then in order to increase the I_{max} of a shaft the amount of cortical material would have to be increased. This is seen to be the case in Fig. 8.

Lateral and dorso-ventral stiffness of the shaft

In feathers other than the outermost feathers on the wing, dorso-ventral exceeded lateral flexural stiffness. This seems quite reasonable, as it would be expected that in flight the greatest forces would act on the shaft in the downstroke, so that the shaft is stiffer in the dorso-ventral direction to resist this. The outermost primary constitutes the leading edge of the wing tip. In flight there are drag forces as well as lift forces generated on any aerofoil. As the other primaries lie behind the leading edge feather and are thus partly shielded by it, it would be good design to incorporate the bulk

of resistance to drag into this outermost feather. This proves to be so, the flexural stiffness in the lateral direction being higher in the outermost feather than in those lying behind it. Examination of the rachis sections shows how this increase of lateral flexural stiffness is achieved; in the outermost feather the width of the section is greater than in feathers proximal to it (see Fig. 4) so that the lateral walls are further from the neutral axis for lateral bending. Consideration of the effect of this on I_{vv} will show that this results in increased flexural stiffness.

Notice that the differential flexural stiffness in the two planes of bending is achieved by a change in morphology rather than a change in the material of the shaft, as might be achieved by varying the cross-link density of the keratin. It is possible that the latter process would embrittle the shaft too much for its mechanical safety, reducing its toughness to the point where it is easily broken.

REFERENCES

ALEXANDER, R. McN. (1968). *Animal Mechanics*. London: Sidgwick & Jackson.

RUTSCHKE, E. (1966). Utersuchungen über die Feinstruktur des Schaftes der Vogelfeder. *Zool. Jb. Syst.* **93**, 223–288.

WAINWRIGHT, S. A., BIGGS, W. D., CURREY, J. D. & GOSLINE, J. M. (1976). *Mechanical Design in Organisms*. London: Edward Arnold.